Morphologic and morphometric magnetic resonance imaging features of Doberman Pinschers with and without clinical signs of cervical spondylomyelopathy

Ronaldo C. da Costa, DMV, PhD; Joane M. Parent, DMV, MVetSc; Gary Partlow, PhD; Howard Dobson, BVM&S, DVSc; David L. Holmberg, DVM; Jonathan LaMarre, DVM, PhD

Objective—To compare morphologic and morphometric features of the cervical vertebral column and spinal cord of Doberman Pinschers with and without clinical signs of cervical spondylomyelopathy (CSM; wobbler syndrome) detected via magnetic resonance imaging (MRI).

Animals—16 clinically normal and 16 CSM-affected Doberman Pinschers.

Procedures—For each dog, MRI of the cervical vertebral column (in neutral and traction positions) was performed. Morphologically, MRI abnormalities were classified according to a spinal cord compression scale. Foraminal stenosis and intervertebral disk degeneration and protrusion were also recorded. Morphometric measurements of the vertebral canal and spinal cord were obtained in sagittal and transverse MRI planes.

Results—4 of 16 clinically normal and 15 of 16 CSM-affected dogs had spinal cord compression. Twelve clinically normal and all CSM-affected dogs had disk degeneration. Foraminal stenosis was detected in 11 clinically normal and 14 CSM-affected dogs. Vertebral canal and spinal cord areas were consistently smaller in CSM-affected dogs, compared with clinically normal dogs. In neutral and traction positions, the intervertebral disks of CSM-affected dogs were wider than those of clinically normal dogs but the amount of disk distraction was similar between groups.

Conclusions and Clinical Relevance—The incidence of intervertebral disk degeneration and foraminal stenosis in clinically normal Doberman Pinschers was high; cervical spinal cord compression may be present without concurrent clinical signs. A combination of static factors (ie, a relatively stenotic vertebral canal and wider intervertebral disks) distinguished CSM-affected dogs from clinically normal dogs and appears to be a key feature in the pathogenesis of CSM. (*Am J Vet Res* 2006;67:1601–1612)

Received December 5, 2005.
Accepted February 15, 2006.

From the Departments of Biomedical Sciences (da Costa, Partlow, LaMarre) and Clinical Studies (Parent, Dobson, Holmberg), Ontario Veterinary College, University of Guelph, Guelph, ON, N1G 2W1, Canada. Dr. da Costa's present address is Universidade Federal do Paraná, Campus Palotina, Palotina, PR, 85950-000, Brazil.

Supported by the Pet Trust Foundation from the Ontario Veterinary College and the Doberman Foundation of America. Dr. da Costa was sponsored by the CNPq–National Scientific Research Council of Brazil.
Presented as an abstract at the 23rd Forum of the American College of Veterinary Internal Medicine, Baltimore, June 2005.
This report represents a portion of a thesis submitted by the first author to the University of Guelph as partial fulfillment for the PhD degree.

Address correspondence to Dr. da Costa.

Abbreviations

CSM	Cervical spondylomyelopathy
MR	Magnetic resonance
CT	Computed tomography
TR	Repetition time
TE	Echo time
FLASH	Fast, low-angle shot
Gd-DTPA	Gadolinium-diethylene triamine pentacetic acid

Cervical spondylomyelopathy, also known as wobbler syndrome, is the most common neurologic disorder of the cervical vertebral column of large-breed dogs. It is characterized by abnormalities of the cervical vertebral column that result in neurologic deficits, cervical hyperesthesia, or both.[1] The disease commonly affects young Great Danes and middle-aged or old Doberman Pinschers.[2-6] Doberman Pinschers are the most commonly affected breed of dog, accounting for as many as 68% of cases.[7] In CSM, both bony and ligamentous abnormalities of the caudal cervical vertebral column develop, causing static and dynamic spinal cord compression. It has been proposed that instability has a primary role in the pathogenesis of CSM.[8,9] In Doberman Pinschers, chronic degenerative disk disease seems to be an important factor, so much so that some authors have suggested the term disk-associated wobbler syndrome.[1,10] Canine CSM has similarities with the cervical spondylotic myelopathy of humans, and the Doberman Pinscher breed has been proposed as a model of naturally occurring disease for investigation of the human condition.[a] There are numerous published articles describing the clinical features and diverse range of treatment methods proposed for CSM, but there is little information regarding its pathogenesis.[3,9,11,12] A lack of knowledge of the cause, pathogenesis, and progression of CSM in dogs remains.

Results of morphometric or quantitative studies[13-17] of the cervical vertebral column in humans involving MR imaging or postmortem examination have been extensively described. Morphometric investigations increase our understanding of spinal diseases by comparing anatomic measurements obtained from clinically normal and affected populations. Postmortem and radiographic morphometric investigations[18-22] of the canine cervical vertebral column have been recently conducted. A few quantitative studies[23-25,b] of the lumbosacral, cervical, and thoracic portions of the vertebral column of dogs have been performed by use of CT

images, but to our knowledge, no morphometric or morphologic investigation of the canine vertebral column has been conducted via MR imaging. In humans, it is well established that vertebral column abnormalities can be detected via imaging techniques in individuals without concomitant clinical signs; this knowledge is essential in selecting a method of treatment.[26-29]

In the present study, we hypothesized that dimensions of the vertebral canal structures as well as their morphologic features differed between clinically normal and CSM-affected dogs. The specific objective of the study of this report was to compare the morphologic and morphometric features of the cervical vertebral column of Doberman Pinschers with and without clinical signs of CSM via MR imaging. The study was part of a larger investigation of the morphologic and morphometric features, electrophysiologic findings,[30] diagnosis, and natural history of Doberman Pinschers with and without signs of CSM.

Materials and Methods

Animals—Two groups of client-owned Doberman Pinschers were prospectively studied. The experiment was conducted in accordance with the guidelines of and by approval of the Animal Care Committee of the University of Guelph. Consent from the owners was obtained prior to study enrollment. The first group consisted of 16 Doberman Pinchers that were defined as clinically normal on the basis of history and results of physical and neurologic examinations, CBC, and serum biochemical analyses. Eight dogs were male and 8 were female. The mean age was 4.3 years (age range, 2 to 8 years); only 3 dogs were older than 6 years of age. The second group of dogs included 16 Doberman Pinschers with clinical signs of CSM (ie, signs of neck pain or neurologic deficits consistent with cervical spinal cord disease). Nine dogs were male and 7 were female. The mean age was 6 years (age range, 3 to 8 years). Physical and neurologic examinations, CBC, and serum biochemical analyses were also performed in all CSM-affected dogs. The time of onset of the clinical signs was recorded. By use of a grading system (modified from that of McKee et al[31]), the neurologic status of the CSM-affected dogs was graded from 1 to 5 as follows: grade 1, cervical hyperesthesia; grade 2, mild pelvic limb ataxia or paresis; grade 3, moderate pelvic limb ataxia or paresis; grade 4, marked pelvic limb ataxia with thoracic limb involvement; and grade 5, tetraparesis or inability to stand or walk without assistance. Prior to study enrollment, electro- and echocardiographic assessments revealed no cardiac abnormalities in any clinically normal or CSM-affected dog.

MR imaging protocol—For MR imaging, the dogs were anesthetized with propofol and isoflurane. They were positioned in dorsal recumbency. Magnetic resonance imaging was performed with a 1.5-T magnet[c] and a circular polarized cervical vertebral column array coil. The field of view was constant for all dogs (25 cm in the sagittal plane and 16 cm in the transverse plane). Two acquisitions (number of excitations [Nex]) were obtained for each imaging sequence. A matrix size of 256 × 256 voxels was used for all sections, and the slice thickness was 3 mm with no interslice space for all sequences. Settings used for sagittal MR imaging were as follows: T1 weighted (TR = 600 milliseconds; TE = 20 milliseconds), turbo spin echo-T2 weighted (TR = 4,620 milliseconds; TE = 120 milliseconds), proton density weighted (TR = 4,620 milliseconds; TE = 20 milliseconds), and inversion recovery weighted (TR = 2,200 milliseconds; TE = 14 milliseconds). Images were acquired in the transverse plane and included T1-, T2-, and proton density–weighted and gradient echo–FLASH images (TR = 672 milliseconds; TE = 15 milliseconds; and flip angle, 30°) combined with magnetization transfer, with and without IV injection of dogs with Gd-DTPA[d] (0.1 mmol/kg). Settings used for transverse T1-, T2-, and proton density–weighted images were similar to those used in the sagittal plane. The dorsal images were acquired as T1-weighted images only.

After acquisition of all image sequences with the cervical area in neutral position, images were acquired as linear traction was applied on the cervical vertebral column by use of a neck harness and weight designed to exert 9-kg traction. The kinematic (traction) images were acquired via sagittal turbo spin echo-T2–weighted imaging. The area of imaging extended from the first cervical vertebra to the second thoracic vertebra and included all 6 intervertebral disks (C2-3, C3-4, C4-5, C5-6, C6-7, and C7-T1). The transverse slices were set parallel to each intervertebral disk and arranged to pass through the centers of the disks and the cranial and caudal vertebral end plates. Each intervertebral disk region had 5 transverse sections; for each dog, 30 transverse images were obtained in each imaging sequence (T1-, T2-, and proton density–weighted images and gradient echo–FLASH images combined with magnetization transfer, with and without IV administration of Gd-DTPA to dogs), resulting in 150 images in the transverse plane/dog. To avoid variations in image interpretation, all images were printed with a laser film printer at a magnification of 1.25×. The printout films had 20 images (4 images/row; 5 images/column) in the transverse plane and 12 images (4 images/row; 3 images/column) in the sagittal plane.

Qualitative analysis of MR images—On the midsagittal T2-weighted images, each disk space was classified according to a modified spinal cord compression scale[32] as follows: grade 0, no compression; grade 1, partial subarachnoid space compression; grade 2, complete subarachnoid space compression; and grade 3, spinal cord compression **(Figure 1)**. The transverse images were used in association with the sagittal images to confirm these spinal cord abnormalities. Spinal cord MR signal changes were evaluated on the sagittal T2-, T1-, and inversion recovery–weighted images. Abnormal spinal cord signal intensities were classified as hyperintense or hypointense, compared with the areas of normal spinal cord signal intensity cranial and caudal to the abnormality on each imaging sequence. Each intervertebral disk was classified as normal, partially degenerated, or completely degenerated on the basis of signal intensities evident on midsagittal T2-weighted images. A normal signal was

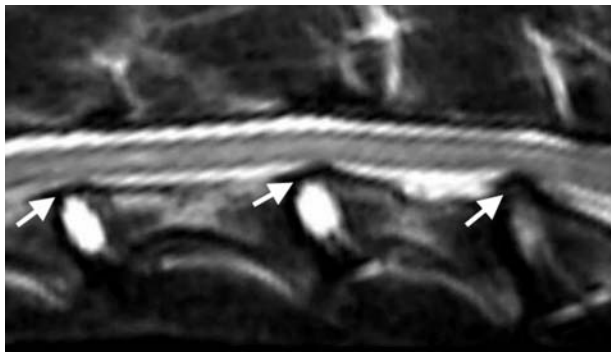

Figure 1—Sagittal T2-weighted (TR = 4,620 milliseconds; TE = 120 milliseconds) MR image at the cervical level of the vertebral column of a Doberman Pinscher with CSM. At each of 3 disk spaces, compression was classified as partial subarachnoid space compression (grade 1 [arrow far left]); complete subarachnoid space compression (grade 2 [arrow middle]); and spinal cord compression (grade 3 [arrow far right]).

assumed when the disk had a uniform high signal; partial degeneration was assumed when part of the disk had evidence of hypointensity; and total disk degeneration was assumed when the entire disk was hypointense.

The degree of disk protrusion was also assessed on the midsagittal and transverse T1- and T2-weighted images and subjectively classified as normal or mild, moderate, or marked herniation (protrusion or extrusion). The severity of the herniation was determined on the basis of the amount of disk displacement in relation to the cranial and caudal end plates in the sagittal images. Foraminal stenosis was evaluated on the transverse gradient echo-FLASH images combined with magnetization transfer that were obtained after IV administration of Gd-DTPA to dogs; the images were centered at the disk space. Foraminal stenosis was subjectively classified as absent, mild, moderate, or severe on the basis of the size and shape of the foramina. The shape and size of each foramen were assessed comparatively, but the decision as to whether it was normal or stenotic was made on the basis of the expected normal morphologic foraminal appearance at a given level. Spondylosis or signal changes in the cranial and caudal end plates were also recorded from the sagittal T1-, T2-, and proton density–weighted images.

Morphometric analysis of MR images—The morphometric analysis was performed by use of a computer software program for image analysis.[e] On the midsagittal T2-weighted images, the spinal cord and the vertebral canal diameter (height) were measured at the cranial aspect of each vertebral body (vertebral level) and at each intervertebral disk level from C2-3 to C7-T1 **(Figure 2)**. Before and after application of traction, intervertebral disk spaces (width) were measured from C2-3 to C7-T1 on the midsagittal T2-weighted images. On the transverse T2-weighted images, the vertebral canal and spinal cord areas, heights, and widths were also measured at the cranial aspect of each vertebral body (vertebral level) and each intervertebral disk (disk level) from C2 to C7-T1. By dividing the height by the width (height-to-width ratio), an approximate roundness index of the spinal cord and vertebral canal was obtained for each region. The proportion of the vertebral canal occupied by the spinal cord was determined by dividing the area of the spinal cord by the area of the vertebral canal and multiplying by 100. The middle foraminal height of each intervertebral foramen was measured on the transverse gradient echo–FLASH images combined with magnetization transfer that were obtained after IV administration of Gd-DTPA to dogs. All foraminal measurements were performed on the transverse section centered at the disk space, with the high signal intensity of the articular facet as reference. The same investigator (RCdC) performed all measurements. One hundred twenty measurements were performed for each dog—36 in the sagittal plane and 84 in the transverse plane.

Data analysis—Statistical analyses of the morphologic data were performed by use of a Wilcoxon Mann-Whitney test. Morphometric data were analyzed by use of a 2-way ANOVA, with group (clinically normal or CSM-affected) and location (vertebral or disk level) as variables. Post hoc Tukey tests were used to correct for multiple comparisons when the overall *F* test was significant.

Logarithmic transformation was used to normalize the data and fulfill the assumptions of ANOVA for results of the height of the vertebral canal at the vertebral level in the sagittal and transverse planes. Analyses were performed by use of computer software.[f] Significance was established at a value of $P < 0.05$.

Results

Historical and neurologic findings—Unaffected dogs were identified as clinically normal on the basis of results of physical and neurologic examinations, CBC, and serum biochemical analyses and the absence of historical findings suggestive of spinal cord disease. Histories of the CSM-affected dogs indicated that 5 dogs had a sudden onset of clinical signs, 9 dogs had a chronic progression of signs, and 2 dogs had an acute worsening of chronic signs. Neurologically, the CSM-affected dogs were graded as the following: grade 1 (cervical hyperesthesia), 3 dogs; grade 2 (mild ataxia), 2 dogs; grade 3 (moderate ataxia), 4 dogs; grade 4 (severe ataxia), 6 dogs; and grade 5 (nonambulatory), 1 dog. A posture with elbow abduction and internal rotation of thoracic limb digits (so-called toe-in posture) was observed in 7 CSM-affected and 8 clinically normal dogs.

Spinal compression scale—On the basis of the worst compression detected in each clinically normal

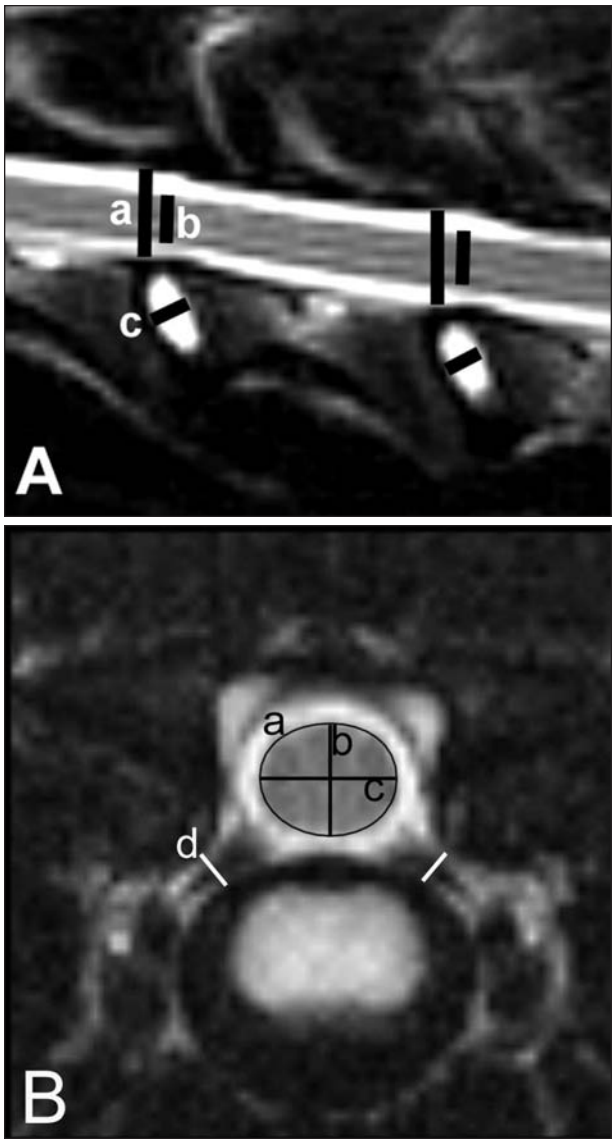

Figure 2—Sagittal and transverse T2-weighted (TR = 4,620 milliseconds; TE = 120 milliseconds) MR images at the cervical level of the vertebral column of a clinically normal Doberman Pinscher. A—Sagittal location of the measurements: height of the vertebral canal (a), height of the spinal cord (b), and width of the intervertebral disk (c). B—Transverse location of the measurements: area of the spinal cord (a), height of the spinal cord (b), width of the spinal cord (c), and middle foraminal height (d).

dog, 8 dogs had partial subarachnoid space compression, 4 dogs had complete subarachnoid space compression, and 4 dogs had spinal cord compression. On analysis of all disk regions in all clinically normal dogs (6 disks for each of 16 dogs), 60 of 96 (62.5%) disk regions were abnormal; these included 49 partial subarachnoid compressions (16 dogs), 7 complete subarachnoid compressions (5 dogs), and 4 spinal cord compressions (4 dogs). The disk regions that were more commonly affected (in decreasing order) were C3-4 and C4-5 (14 dogs each), C6-7 and C2-3 (11 dogs each), and C5-6 (10 dogs). Spinal cord signal abnormalities were not detected in clinically normal dogs.

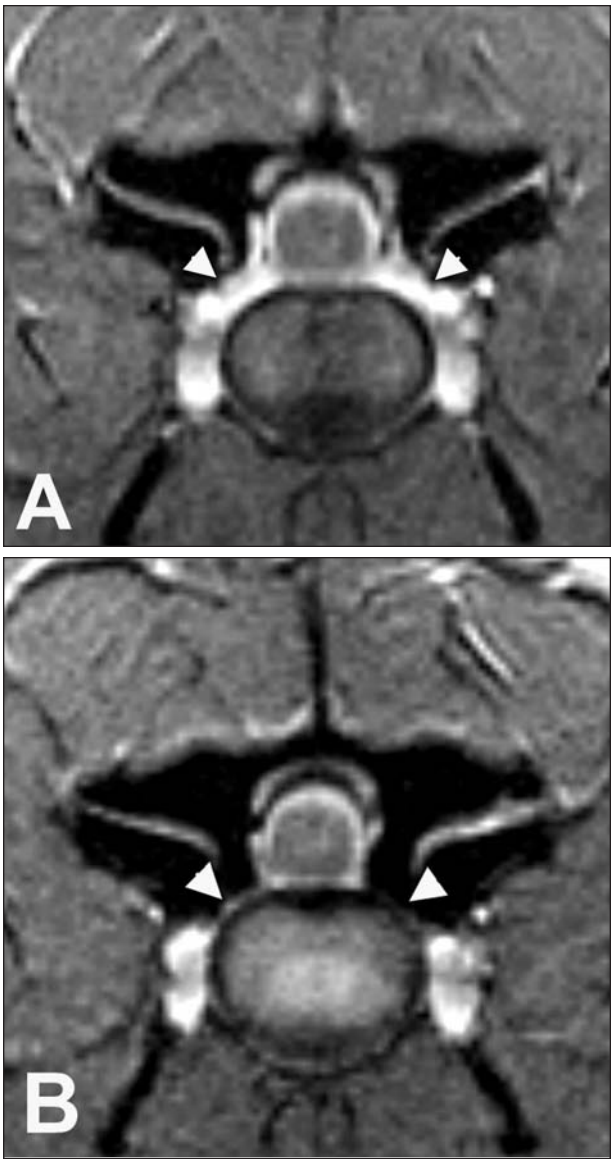

Figure 3—Transverse gradient echo-FLASH (TR = 672 milliseconds; TE = 15 milliseconds) MR images with magnetization transfer obtained at the level of the C4-5 intervertebral disk in 2 dogs after IV administration of Gd-DPTA. A—Image from a 2 year-old female spayed clinically normal Doberman Pinscher. Notice the intervertebral foramina, which are classified as normal (arrowheads). B—Image from another 2-year-old female spayed clinically normal Doberman Pinscher. Marked foraminal stenosis is evident bilaterally (arrowheads).

On the basis of the worst compression detected in each of the CSM-affected dogs, 1 dog had partial subarachnoid space compression and 15 dogs had spinal cord compression. On analysis of all disk regions in all CSM-affected dogs, 68 of 96 (71%) disk regions were abnormal; these included 44 partial subarachnoid space compressions (n = 15 dogs), 5 complete subarachnoid space compressions (6), and 19 spinal cord compressions (15; 3 dogs had > 1 area of spinal cord compression). The disk regions that were more commonly affected (in decreasing order) were C4-5 and C5-6 (n = 15 dogs each), C3-4 (14), C6-7 (13), and C2-3 (11). Nine dogs had spinal cord signal abnormalities at the site of compression; hyperintensity of the spinal cord was detected in the T2-weighted images of all dogs, and hypointensity of the spinal cord was detected in the T1-weighted images of 1 dog. Statistical comparison of the results of spinal cord compression gradings indicated that the cumulative scores for the 2 groups were significantly (P = 0.025) different. The cause of clinical signs in the 16 CSM-affected dogs was assumed to be disk related in 14 dogs; associated with foraminal stenosis in 1 dog (which had signs of neck pain only); and attributable to articular facet impingement, causing bilateral spinal cord compression, in another dog. Compression of the spinal cord secondary to solely hypertrophied ligaments was not detected in any CSM-affected dog.

Intervertebral disk degeneration—In the 16 clinically normal dogs, 12 had disk degeneration; multiple disks were affected in 11 dogs. Among the 96 disks examined in all clinically normal dogs, 31 were degenerated; of these, 17 were partially degenerated (n = 10 dogs) and 14 were completely degenerated (7). The disks that were more often involved were C6-7 (n = 11 dogs) and C5-6 and C7-T1 (8 each). Among the CSM-affected dogs, all had disk degeneration. In 14 dogs, multiple disks were involved, whereas in 2 dogs, 1 disk was affected. Among the 96 disks examined in all CSM-affected dogs, 46 were degenerated; the degeneration was classified as partial in 25 disks (n = 12 dogs) and complete in 21 disks (14). Disk degeneration was detected more commonly (in decreasing order) at C6-7 (n = 15), C5-6 (13), C7-T1 (10), and C4-5 (7). There

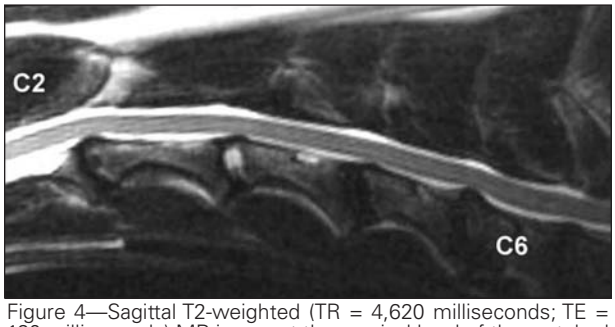

Figure 4—Sagittal T2-weighted (TR = 4,620 milliseconds; TE = 120 milliseconds) MR image at the cervical level of the vertebral column of a clinically normal 7-year-old, neutered male Doberman Pinscher. Notice the complete disk degeneration in all disks of the cervical portion of the vertebral column except for the C3-4 disk, which is partially degenerated. Mild spinal cord compression is detectable at disk space C5-6. C2 and C6 = Second and sixth cervical vertebrae, respectively.

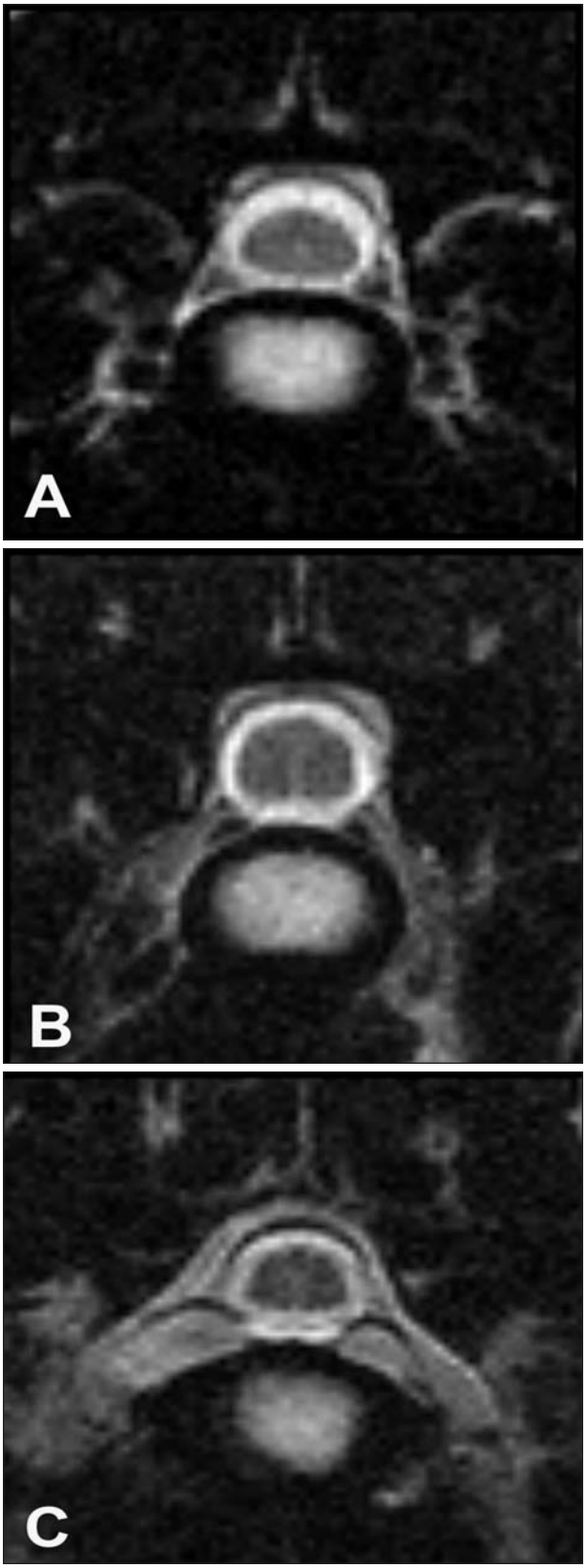

Figure 5—Transverse T2-weighted (TR = 4,620 milliseconds; TE = 120 milliseconds) MR images at the level of the C2-3 (A), C5-6 (B), and C7-T1 (C) intervertebral disks of a clinically normal Doberman Pinscher. Notice the different shapes of the spinal cord at each cervical level. The normal spinal cord at C7-T1 assumes a trapezoid shape.

was a significant ($P = 0.04$) difference in the incidence of disk degeneration between the clinically normal and CSM-affected groups.

Intervertebral disk protrusion—All clinically normal dogs had some degree of disk protrusion, which was considered mild in 11 dogs, moderate in 2 dogs, and severe in 3 dogs. Twelve dogs had multiple disks affected, whereas 4 dogs each had only 1 disk affected. Among the 96 disks examined in all clinically normal dogs, 46 were associated with protrusion, which was categorized as mild, moderate, and severe for 39 (n = 16 dogs), 3 (4), and 4 (3) disks, respectively. The highest incidence of protrusion was observed at C4-5 (n = 11 dogs), followed (in decreasing order) by C3-4, C5-6, and C6-7 (8 each) and C2-3 and C7-T1 (2 each).

Findings in the CSM-affected dogs were similar to those in clinically normal dogs, in that all dogs had disk protrusion. However, the overall extent of this abnormality was more severe in CSM-affected dogs; protrusion was considered mild in 1 dog, moderate in 2 dogs, and severe in 13 dogs. All 16 CSM-affected dogs had multiple disk protrusions. Among the 96 disks examined in all CSM-affected dogs, 62 were associated with protrusion, which was categorized as mild, moderate, and severe in 36 (n = 15 dogs), 13 (11), and 13 (13) disks, respectively. Intervertebral disks C5-6 and C6-7 were affected in all 16 dogs, followed (in decreasing order) by C4-5 (n = 13 dogs), C3-4 (11), C2-3 (5), and C7-T1 (1). There was a significant ($P = 0.007$) difference in the incidence of disk protrusion between the clinically normal and CSM-affected groups.

Foraminal stenosis—Eleven clinically normal dogs had foraminal stenosis that was graded as moderate in 8 dogs, severe in 2 dogs, and mild in 1 dog **(Figure 3)**. In 8 dogs, multiple foramina were affected, whereas in each of 3 dogs, a single foramen was involved. Because most dogs had similar changes bilaterally, we considered both left and right foramina as 1 unit. On analysis of all foramina of all clinically normal dogs, it was determined that 21 of 96 (22%) had some degree of stenosis, which was categorized as mild (n = 7 dogs), moderate (11), and severe (3). The foramen at C6-7 was the most commonly affected site (n = 10 dogs), followed (in decreasing order) by the foramina at C5-6 (8), C3-4 (2), and C4-5 (1). One dog had marked osteoarthritic changes in the articular processes that resulted in foraminal stenosis at C4-5, C5-6, and C6-7.

Fourteen CSM-affected dogs had foraminal stenosis; multiple sites were affected in 8 dogs, and a single site was affected in each of 6 dogs. The stenosis was categorized as severe in 6 dogs and mild or moderate in 4 dogs each. On analysis of all intervertebral foramina of all CSM-affected dogs, 22 of 96 (23%) had stenosis, which was categorized as mild in 7 foramina (n = 7 dogs), moderate in 9 foramina (7), and severe in 6 foramina (6). The foramen at C6-7 was affected in 11 dogs, followed (in decreasing order) by the foramina at C5-6 (n = 10

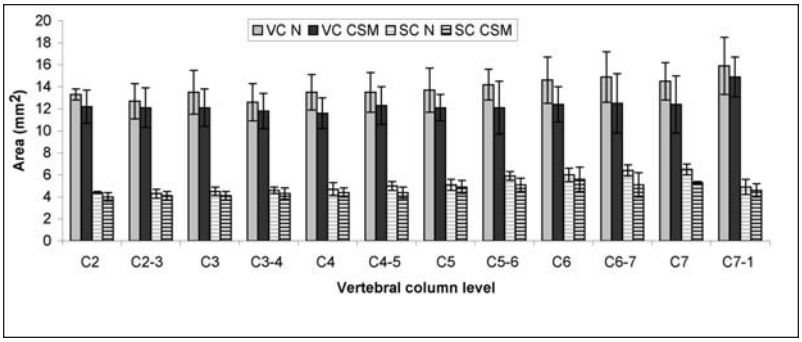

Figure 6—Mean ± SD area (transverse MR image plane) of the vertebral canal and spinal cord at the levels of the vertebral bodies and intervertebral disks in the cervical portion of the vertebral column in clinically normal (n = 16) and CSM-affected (16) Doberman Pinschers. Compared with findings in clinically normal Doberman Pinschers, the areas of the vertebral canal and spinal cord of CSM-affected Doberman Pinchers were significantly ($P < 0.05$) smaller at both the vertebral and intervertebral disk levels. VC = Vertebral canal. N = Clinically normal Doberman Pinschers. CSM = Doberman Pinschers clinically affected with CSM. SC = Spinal cord.

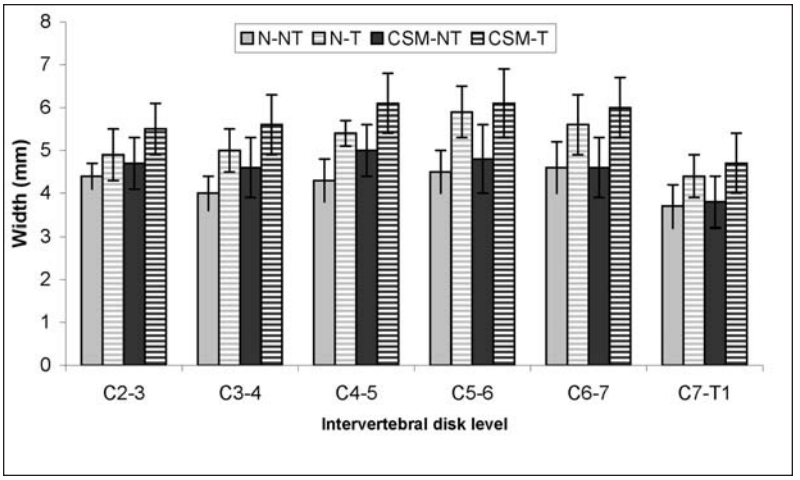

Figure 7—Mean ± SD width (sagittal MR image plane) of intervertebral disks in the cervical portion of the vertebral column (with and without traction) in clinically normal (n = 16) and CSM-affected (16) Doberman Pinschers. Intervertebral disk widths with and without traction were significantly ($P < 0.05$) different between groups, but the amount of disk distraction was not different ($P > 0.05$) between groups. N-NT = Disks in clinically normal dogs without traction. N-T = Disks in clinically normal dogs with traction. CSM-NT = Disks in CSM-affected dogs without traction. CSM-T = Disks in CSM-affected dogs with traction.

dogs) and C2-3 (1). No significant ($P = 0.80$) difference in the incidence of foraminal stenosis was detected between the clinically normal and CSM-affected groups.

Other pathologic changes—End-plate sclerosis, which appeared as a linear, regular, or irregular area of hypointensity on the sagittal T1- and T2-weighted images, was identified in 4 clinically normal and 6 CSM-affected Doberman Pinschers. End-plate sclerosis affected the C6-7 disk region in all dogs, being more visible at the caudal end plate of C6. One clinically normal dog had end-plate changes at disk regions C4-5, C5-6, and C6-7, with spondylosis at C6-7, whereas the most severe disk protrusion was at C5-6 (**Figure 4**). Three CSM-affected dogs had spondylosis located at C6-7; one of those dogs also had spondylosis at C7-T1. Tipping or tilting of the vertebral body was observed in images of 3 clinically normal dogs and 7 dogs with CSM. The spinal cord shape in both groups of dogs varied according to the region. At the C2-3 and C3-4 disk levels, the spinal cord appeared as a flattened ellipse dorsoventrally, whereas at the C4-5, C5-6, and C6-7 disk levels, it had the appearance of a less flattened and more circular ellipse; at the C7-T1 disk level, it often had a trapezoid shape (**Figure 5**). One clinically normal dog had a mild syringohydromyelia in the cervical spinal cord from vertebrae C2 through C4. An MR image scan of the head was performed after the syrinx was identified, but no abnormalities were detected in either the brain or cervical vertebral column to account for this anomaly.

Morphometric data—Overall, 3,795 measurements of the vertebral column and spinal cord were obtained from 32 dogs. It was not possible to measure the intervertebral disk space width in 45 completely degenerated intervertebral disks because the distinction between disk and end plate was obscured and an accurate measurement could not be performed. Intervertebral disk space width was not available for 27 disks of 9 clinically normal dogs (12 disks at C7-T1, 7 disks at C6-7, and the remainder distributed among more cranial disk sites) and 18 disks of 14 CSM-affected dogs (8 disks at C6-7, 7 disks at C7-T1, and the remainder distributed among more cranial disk sites). In 2 dogs of the clinically normal group, all 6 disks of their cervical vertebral columns were totally degenerated, which contributed to the higher proportion of degenerated disks that could not be measured in clinically normal dogs.

The area of the vertebral canal at all levels in CSM-affected dogs was significantly smaller than corresponding areas in the clinically normal dogs (disk level, $P = 0.006$; vertebral level, $P < 0.001$; **Figure 6**). Similarly, the area of the spinal cord at all levels in CSM-affected dogs was also significantly smaller than corresponding areas in the clinically normal dogs (disk level, $P < 0.001$; vertebral level, $P = 0.004$).

The mean width of intervertebral disk spaces without traction was 4.31 mm in clinically normal dogs and 4.66 mm in CSM-affected dogs; these values were significantly ($P = 0.036$) different between groups (**Figure 7**). With application of traction, the mean width of disk spaces in clinically normal and CSM-affected dogs was 5.29 and 5.75 mm, respectively; these values were also significantly ($P = 0.022$) different between groups. When the difference between the post-traction and pretraction measurements was taken into account, the

mean percentage of disk space distraction in clinically normal dogs was 22.7%, whereas in CSM-affected dogs, it was 23.3%; these values were not different (P = 0.448) between groups. Because of their clinical importance, we also analyzed the caudal cervical disk spaces (C4-5, C5-6, and C6-7) separately; the mean percentage of distraction was 26.4% in clinically normal dogs and 26.5% in CSM-affected dogs.

The mean and SD values for the linear measurements (height and width) of the vertebral canal and spinal cord were calculated (**Table 1**). The overall results for the height of the vertebral canal in the sagittal plane, at the disk and vertebral levels, were not significantly different between the clinically normal and CSM-affected groups, but there was a difference in heights at disk levels C5-6 (P = 0.027) and C6-7 (P = 0.003) between groups. Results for the height of the spinal cord in the sagittal plane were significantly different between groups at the disk ($P < 0.001$) and vertebral (P = 0.004) levels.

Heights of the vertebral canal in the transverse plane were different between groups at the vertebral levels (P = 0.012) but not at the disk levels (P = 0.060). Results for the height of the spinal cord in the transverse plane were different between groups at both the disk (P = 0.014) and vertebral (P = 0.023) levels. Widths of the vertebral canal in the transverse plane were not significantly different between groups. Results for the width of the spinal cord in the transverse plane were different between groups at both the disk (P = 0.049) and vertebral (P = 0.015) levels.

The height-to-width ratios (approximate roundness index) of the transverse aspect of the vertebral canal and spinal cord were each calculated (**Table 2**). The height-to-width ratio of the vertebral canal was different between groups when measured at the vertebral level (P = 0.042) but not at the disk level. There was no difference in height-to-width ratio of the spinal cord in the transverse plane between groups.

From the C2 vertebra to C4-5 disk space, the mean proportion of the vertebral canal occupied by the spinal cord was 34.6% in clinically normal dogs (range, 33% to 37%) and 35.1% in CSM-affected dogs (range, 33% to 38%). In the caudal cervical area (C5 to C7), the cord occupied 41.4% and 42.2% of the vertebral canal in clinically normal and CSM-affected dogs, respectively. At the C7-T1 disk region, the spinal cord occupied 31% of the vertebral canal in both groups (Table 2).

Because results of the foraminal measurements revealed no significant difference between left and right sides, both sides were grouped for analysis. There

Table 1—Morphometric MR imaging results (sagittal and transverse planes) of the height and width of the vertebral canal and spinal cord in clinically normal Doberman Pinschers (n = 16) and Doberman Pinschers with clinical signs of CSM (16).

Level*	Dogs	Sagittal vertebral canal height (mm)	Sagittal spinal cord height (mm)	Transverse vertebral canal height (mm)	Transverse vertebral canal width (mm)	Transverse vertebral spinal cord height (mm)	Transverse vertebral spinal cord width (mm)
C2	Clinically normal	10.5 ± 0.8	4.9 ± 0.5	11.6 ± 0.8	12.5 ± 0.7	5.9 ± 0.6	7.9 ± 0.6
	CSM affected	10.2 ± 0.5	4.5 ± 0.5	11.2 ± 0.9	12.3 ± 0.9	5.6 ± 0.4	7.9 ± 0.5
C2-3	Clinically normal	9.7 ± 0.9	4.8 ± 0.6	11.0 ± 1.1	13.2 ± 1.3	5.6 ± 0.4	8.0 ± 0.5
	CSM affected	9.4 ± 0.9	4.4 ± 0.5	10.8 ± 0.9	13.5 ± 1.3	5.7 ± 0.5	8.0 ± 0.4
C3	Clinically normal	9.8 ± 0.5	5.0 ± 0.1	11.8 ± 1.2	13.4 ± 1.4	5.9 ± 0.5	8.1 ± 0.5
	CSM affected	9.3 ± 0.8	4.5 ± 0.5	11.0 ± 1.2	13.3 ± 0.9	5.6 ± 0.5	7.6 ± 0.4
C3-4	Clinically normal	8.6 ± 0.9	4.9 ± 0.3	9.9 ± 0.9	13.6 ± 1.2	5.6 ± 0.6	8.2 ± 0.3
	CSM affected	8.6 ± 0.9	4.2 ± 0.7	9.7 ± 1.1	13.6 ± 0.8	5.3 ± 0.7	7.9 ± 0.6
C4	Clinically normal	8.3 ± 0.8	4.8 ± 0.3	10.1 ± 0.9	14.6 ± 1.7	5.7 ± 0.6	8.5 ± 0.5
	CSM affected	8.3 ± 0.9	4.3 ± 0.7	9.6 ± 1.2	14.0 ± 1.6	5.5 ± 0.4	8.0 ± 0.5
C4-5	Clinically normal	8.4 ± 1.0	5.0 ± 0.4	10.1 ± 1.2	14.1 ± 1.5	6.0 ± 0.6	8.5 ± 0.6
	CSM affected	8.4 ± 1.2	4.4 ± 0.8	9.4 ± 1.1	13.8 ± 1.0	5.5 ± 0.6	8.2 ± 0.6
C5	Clinically normal	8.7 ± 0.8	5.1 ± 0.5	10.4 ± 1.3	14.4 ± 2.0	6.0 ± 0.7	8.5 ± 0.6
	CSM affected	8.9 ± 0.9	4.6 ± 0.6	9.7 ± 1.0	14.2 ± 1.6	5.9 ± 0.6	8.4 ± 0.8
C5-6	Clinically normal	8.6 ± 1.0	5.5 ± 0.7	10.3 ± 1.1	14.1 ± 1.2	6.5 ± 0.9	9.2 ± 0.7
	CSM affected	7.7 ± 1.3	4.8 ± 1.1	9.0 ± 1.5	13.7 ± 1.3	5.7 ± 0.8	8.9 ± 0.9
C6	Clinically normal	9.7 ± 0.9	6.0 ± 0.5	11.6 ± 1.3	14.2 ± 1.4	6.9 ± 0.7	9.3 ± 0.6
	CSM affected	9.2 ± 0.5	5.6 ± 0.6	10.1 ± 0.8	13.9 ± 1.0	6.3 ± 0.8	8.8 ± 1.1
C6-7	Clinically normal	9.8 ± 1.1	6.2 ± 0.8	11.0 ± 1.5	14.8 ± 1.0	6.9 ± 0.7	9.5 ± 0.7
	CSM affected	8.5 ± 2.3	5.2 ± 1.5	10.2 ± 1.7	13.5 ± 0.4	5.9 ± 1.0	8.6 ± 1.3
C7	Clinically normal	9.8 ± 0.6	6.0 ± 0.6	11.7 ± 1.4	14.3 ± 1.1	7.0 ± 0.4	9.6 ± 0.5
	CSM affected	9.5 ± 0.1	5.7 ± 0.9	10.4 ± 1.7	14.0 ± 1.7	6.1 ± 1.1	8.7 ± 1.2
C7-T1	Clinically normal	10.6 ± 0.7	5.9 ± 0.7	13.2 ± 1.4	14.4 ± 1.4	6.6 ± 0.5	7.8 ± 0.7
	CSM affected	10.8 ± 0.9	5.3 ± 0.7	13.0 ± 1.1	14.4 ± 1.1	6.4 ± 0.8	7.6 ± 0.5

Data are presented as mean ± SD.
*Levels refer to the vertebral body level or intervertebral disk level in a craniocaudal sequence.

Table 2—Morphometric MR imaging results of the height–to-width ratios (approximate roundness index) of the vertebral canal and spinal cord, proportion of the vertebral canal area occupied by the spinal cord, and middle foraminal height in clinically normal Doberman Pinschers (n = 16) and Doberman Pinschers with clinical signs of CSM (16).

Level*	Dogs	Height-to-width ratio of vertebral canal	Height-to-width ratio of spinal cord	Proportion of vertebral canal occupied by spinal cord (%)	Foraminal height (mm)
C2	Clinically normal	9.2 ± 0.7	7.5 ± 1.0	33	NA
	CSM affected	9.2 ± 0.9	7.1 ± 0.5	32	NA
C2-3	Clinically normal	8.3 ± 0.9	7.0 ± 0.7	33	4.3 ± 0.9
	CSM affected	8.0 ± 0.9	7.1 ± 0.7	33	4.4 ± 0.8
C3	Clinically normal	8.8 ± 0.9	7.3 ± 0.8	33	NA
	CSM affected	8.2 ± 0.8	7.3 ± 0.6	33	NA
C3-4	Clinically normal	7.3 ± 0.6	6.9 ± 0.7	36	3.9 ± 0.6
	CSM affected	7.2 ± 0.9	6.7 ± 0.9	36	3.3 ± 0.9
C4	Clinically normal	7.0 ± 1.2	6.7 ± 0.9	34	NA
	CSM affected	6.9 ± 1.1	6.9 ± 0.7	37	NA
C4-5	Clinically normal	7.2 ± 1.3	7.1 ± 1.1	37	3.7 ± 0.6
	CSM affected	6.8 ± 0.9	6.7 ± 1.0	35	3.4 ± 0.9
C5	Clinically normal	7.0 ± 0.7	7.1 ± 1.2	37	NA
	CSM affected	6.8 ± 0.8	7.1 ± 0.9	40	NA
C5-6	Clinically normal	7.4 ± 1.3	7.1 ± 1.3	41	2.3 ± 0.8
	CSM affected	6.6 ± 1.4	6.5 ± 1.3	42	2.6 ± 1.1
C6	Clinically normal	8.2 ± 1.2	7.4 ± 1.1	41	NA
	CSM affected	7.2 ± 0.6	7.1 ± 0.9	45	NA
C6-7	Clinically normal	7.4 ± 1.2	7.3 ± 1.2	42	2.3 ± 1.1
	CSM affected	7.6 ± 1.4	7.0 ± 1.3	40	2.9 ± 1.0
C7	Clinically normal	8.2 ± 1.2	7.3 ± 0.7	44	NA
	CSM affected	7.4 ± 0.8	7.1 ± 1.6	42	NA
C7-T1	Clinically normal	9.1 ± 0.8	8.5 ± 0.6	30	5.4 ± 1.1
	CSM affected	9.5 ± 1.3	8.3 ± 1.1	30	5.3 ± 1.3

NA = Not applicable. *See* Table 1 for key.

was no difference in the middle foraminal height between groups; however, a difference ($P = 0.001$) was detected with regard to level, and the largest foramen was detected at C7-T1, and the 2 smallest foramina were detected at C5-6 and C6-7 (Table 2).

Discussion

In the present study, the morphologic and morphometric features of the cervical vertebral column of clinically normal and CSM-affected Doberman Pinschers were investigated. It was a surprising finding that a high percentage of clinically normal Doberman Pinschers had severe abnormalities of the cervical vertebral column, such as spinal cord compression, intervertebral disk degeneration or protrusion, and foraminal stenosis, all of which are considered as clinically relevant in veterinary practice. In some instances, the MR image abnormalities of clinically normal dogs were more severe than those of CSM-affected Doberman Pinschers with cervical hyperesthesia or mild ataxia. Intervertebral disk degeneration was detected in 12 of 16 clinically normal Doberman Pinschers, and multiple disks were affected in 11 of those 12 dogs. Disk protrusion or herniation was also detected in all clinically normal study dogs. Typically, the protrusions were mild, causing only partial compression of the subarachnoid space; however, more severe protrusions that caused spinal cord compression were present in 4 of the 16 clinically normal dogs. Radiographically, it has been estimated that approximately 25% of clinically normal Doberman Pinschers have vertebral column abnormalities comparable to those detected in dogs with CSM.[6,33] In another study,[34] subclinical abnormalities of the lumbosacral vertebral column were detected via CT in 5 of 6 dogs that were older than 5 years of age (mean age, 8.3 years). In contrast to those changes at the lumbosacral region of the vertebral column, only 1 of 4 clinically normal Doberman Pinschers with cervical spinal cord compression in our study was older than 6 years (the other dogs being ≤ 5 years old). Results of the present study are in partial agreement with findings in humans. Asymptomatic intervertebral disk degeneration and protrusion progressively increase with age in humans, affecting as many as 87% of patients that are more than 60 years of age.[27-29] Asymptomatic spinal cord compression has been identified in 21% of humans undergoing myelography,[26] 29% of patients undergoing CT myelography,[35] and 7.6% of patients undergoing MR imaging.[29] Among the dogs of our study, disk degeneration affected those that

were 2 to 8 years old; even though the study population was relatively small, older dogs seemed to have a higher incidence of disk degeneration. Although disk degeneration per se does not usually result in clinical signs, it is generally accepted as a sine qua non condition that predisposes patients to future disk herniations. However, results of the present study may not represent the real incidence of these abnormalities in the general canine population, because we investigated a breed with a high incidence of abnormalities in the cervical vertebral column. The findings of our investigation indicate that extreme care should be exercised when attributing clinical importance to intervertebral disk degeneration and mild spinal cord compression in Doberman Pinschers. This has to be taken into consideration when planning surgery in dogs with apparently multiple lesions. In corroboration of previous descriptions,[1,31] intervertebral disk protrusion or extrusion, with or without other associated changes, appeared to be the cause of clinical signs in most CSM-affected Doberman Pinchers in the study of this report.

From all morphometric data obtained, the cross-sectional area of the vertebral canal appeared to be one of the consistent findings that distinguished CSM-affected from clinically normal Doberman Pinschers. Based on the evaluation of the vertebral canal area, we determined that the vertebral canal of CSM-affected Doberman Pinschers is stenotic throughout the cervical portion of the vertebral column, not just at the caudal cervical region where most clinical lesions have been detected.[9,36] The vertebral canal of CSM-affected Doberman Pinschers in the present study was smaller even at the C2 and C7-T1 levels, compared with findings in the clinically normal dogs. This finding suggests that CSM-affected Doberman Pinschers have a relative stenosis throughout their cervical vertebral canal. A relative stenosis associated with a space-occupying lesion, such as intervertebral disk disease or articular facet proliferation, could result in the development of clinical signs. In humans, it is well established that a small vertebral canal is an important factor for the development of cervical spondylotic myelopathy,[15,37] and some investigators have suggested that it is the most important static factor.[38,39] A narrow canal lowers the threshold at which the cumulative effects of various structures encroaching on the spinal cord cause signs of myelopathy.[39] A recent ex vivo study[18] revealed that the height of the cranial aspect of the vertebral canal in large-breed dogs is significantly smaller than that in small-breed dogs, resulting in a funnel-shaped vertebral canal particularly within the caudal cervical vertebrae; among the large-breed dogs studied, this funnel-shaped appearance of the vertebral canal was most pronounced in Doberman Pinschers.[18] Based on the proportion of the vertebral canal occupied by the spinal cord determined in the present study, the area available for spinal cord occupancy is smallest at the caudal cervical region of the vertebral canal, where the cervical spinal cord enlargement is located and most compressive lesions develop. On analysis of the findings of our and other investigations, it appears that although Doberman Pinschers have a smaller vertebral canal than other large-breed dogs, CSM-affected Doberman Pinschers have an even more stenotic canal than clinically normal Doberman Pinschers.

In humans, cervical stenosis has been classified as congenital, developmental, and acquired forms.[40] The type of cervical stenosis associated with cervical spondylotic myelopathy of humans is considered acquired. Humans have clinical signs of cervical spondylotic myelopathy only in adult life, whereas Doberman Pinschers, albeit uncommonly, can manifest the disease in the first year of life. In 1 study,[12] a third of Doberman Pinschers examined had abnormally shaped caudal cervical vertebrae before 16 weeks of age. It was suggested that the vertebral changes were congenital or developed in the early postnatal period; however, no follow-up information was available to establish whether those vertebral changes caused clinical signs later in life. Further support for the congenital hypothesis was provided by another study[b] in which abnormalities of the caudal cervical vertebrae and vertebral canal stenosis in neonatal Doberman Pinschers were identified. Other investigators have proposed that the vertebral stenosis of canine CSM is acquired, a result of abnormal stresses placed on the caudal cervical vertebral column (with or without instability).[9]

The spinal cord of CSM-affected Doberman Pinschers was smaller than that of the clinically normal dogs in the present study. Possible causes for this are cord atrophy and Wallerian degeneration cranial and caudal to the compressive site.[41] Spinal cord atrophy has been identified in Doberman Pinschers with CSM via CT myelography[42] and was also evident in the Doberman Pinschers of our study. Overall, the proportion of the vertebral canal occupied by the spinal cord was 38% in the clinically normal dogs and 38.6% in the CSM-affected dogs. One report[43] indicated that the spinal cord occupies 50% of the vertebral canal from vertebra C1 through C3 and 75% of the vertebral canal from vertebrae C5 through C7 in humans; however, in a morphometric MR imaging study,[15] the spinal cord occupied 30.8% to 36.4% of the vertebral canal in clinically normal humans and occupied as much as 40% of the vertebral canal in humans with cervical spondylotic myelopathy. Comparatively, normal Doberman Pinschers have a higher proportion of the vertebral canal occupied by the spinal cord than clinically normal humans.

In the study reported here, the disk distraction measurements indicated that disks of the CSM-affected dogs were significantly wider both with and without traction, compared with findings in clinically normal dogs. This was an unexpected finding because one of the features of disk degeneration is narrowing of the disk space. The wider intervertebral disks of CSM-affected Doberman Pinschers could potentially be at higher risk for herniation. Because they are larger than disks of clinically normal dogs, the volume of disk protrusion into the vertebral canal would be higher than that of normal dogs. This finding, along with a relative canal stenosis, could potentially explain the development of clinical signs in CSM-affected Doberman Pinschers. When the percentages of intervertebral disk distraction were analyzed, no difference was detected

between groups. This finding suggests that the intervertebral disk mobility in the longitudinal plane is similar between clinically normal and CSM-affected Doberman Pinschers, questioning the instability theory for CSM. Although cervical vertebral instability is often mentioned in the veterinary literature,[3,9,44] it has never been objectively evaluated. Instability was initially proposed in the pathogenesis of CSM because of the malalignment of the cervical vertebrae or spinal cord compression that was evident on radiographic views of the cervical portions of large-breed dogs' vertebral columns during flexion and extension.[8,9] Later, results of more objective investigations indicated that slippage of cervical vertebrae and compression of the spinal cord in flexion or extension are evident in all dogs because these represent a natural pattern of motion.[45-47] Read et al[4] investigated 30 dogs with CSM and stated the following in their report: "in many of the cases studied at necropsy, most of the discs in the cervical spine showed varying degrees of degeneration, but instability was only rarely demonstrable." From data collected in an MR imaging study[48] to investigate the relationship between disk degeneration and cervical instability in 260 humans patients, it was concluded that segmental instability was associated with early intervertebral disk degeneration when the image signal was intense or moderately intense.[48] Normal intervertebral disks (very intense signal) and moderate to severely degenerated disks (slight or no hyperintensity) were stable.[48] A finite model further substantiated the relationship between disk degeneration and spinal stability[49]; it was found that the overall and segmental stiffness of the cervical vertebral column increased with increasing severity of disk degeneration.[49] In another study,[50] humans with radiographic evidence of lumbar instability were evaluated with a device fixed to the spinous processes that was able to monitor all kinematic variables; results indicated that the intervertebral range of motion was significantly less (by at least 50%) among patients with disk degeneration, compared with the control group. Because most Doberman Pinschers with CSM have advanced disk degeneration at the time of diagnosis, application of the criteria from human investigations would also not support instability as a mechanism involved in the development of canine CSM.

Foraminal stenosis has been identified as one of the key factors contributing to the ischemic insult in the pathogenesis of cervical spondylotic myelopathy of humans.[43,51] Foraminal nerve root compression can develop secondary to proliferation or subluxation of articular facets, lateralized disk herniation, or osteophyte formation in a vertebral body.[52] In the present study, the incidence of foraminal stenosis in clinically normal dogs (11/16 dogs) and CSM-affected dogs (14/16 dogs) was certainly unexpected. Even though most clinically normal dogs had moderate stenosis, compared with more severe stenosis in CSM-affected dogs, the incidence in that group remains high. There are no data from veterinary studies to compare with this finding; however, the incidence of foraminal stenosis in asymptomatic humans has been reported[28] as 20%. It is unlikely that the MR imaging technique used overestimated foraminal stenosis. The gradient echo image sequence with magnetization transfer has been proposed as the best method for assessment of the intervertebral foramina.[53-55]

A direct correlation between narrowing of disk space and a decrease in foraminal height has been determined in humans[52]; the height of the foramen is less important than its width because the width was consistently smaller in patients with clinical signs versus those without clinical signs.[56] In the present investigation, we measured and classified the foraminal stenosis on the basis of the middle foraminal height, which is equivalent to foraminal width in humans. In both groups of Doberman Pinschers, the intervertebral foraminal height progressively changed caudally along the cervical vertebral column from C2-3, having smaller values at C5-6 and C6-7 and the largest height at C7-T1. To the authors' knowledge, dimensions of intervertebral foramina of other dog breeds have not been described. In clinically normal humans, the width of the intervertebral foramina of the cervical region progressively increases from C3-4 through C7-T1, with C2-3 being as large as C4-5.[57] However, humans with cervical disk degeneration have a progressive decrease in foraminal width from C2-3 through C5-6.[58] We assume that the high incidence of foraminal stenosis in both groups of dogs in the present study was related to disk degeneration, as suggested in humans, because disk degeneration was evident in 12 of the 16 clinically normal Doberman Pinschers. Our measurements were performed while the dogs were positioned in dorsal recumbency with the neck extended. It has been shown in a cadaveric human study[59] that neck flexion increases the dimension of the intervertebral foramen, whereas extension decreases the foraminal dimension by 10% to 13%. A recent in vivo imaging study[60] in humans revealed that cervical extension decreased the foraminal width (the equivalent of foraminal height in dogs) by 22%. We cannot exclude the possibility that the high incidence of foraminal stenosis in the present study was partially caused by the extended neck position used during the scanning process; however, clinically normal Doberman Pinschers typically carry their necks in an extended position. Moreover, dorsal recumbency is the best position in which to place dogs with a deep chest such as Doberman Pinschers to perform scans of the cervical vertebral column. It is possible that marked foraminal stenosis contributes to the pathogenesis of canine CSM by causing local neuroischemia; however, on the basis of our findings in clinically normal Doberman Pinschers, the stenosis has to be very severe for this to occur in this breed of dog. Further studies involving other dog breeds and different neck positions are necessary to resolve the issue of foraminal stenosis in dogs.

Medial proliferation of the articular facets causing spinal cord compression is evident more often in giant breeds of dogs than large breeds.[61] However, it was also detected in 1 Doberman Pinscher with CSM in the present study. Although the disease in Doberman Pinschers is primarily disk related, an overlap between the pathologic changes of large- and giant-breed dogs seems to exist.

The height-to-width ratios of the vertebral canal and spinal cord have been extensively used to assess morphometric changes in humans and dogs.[13,14,62,63] Interestingly, in the present study, the ratios were not consistently different between groups, whereas measurements of the areas of the vertebral canal and spinal cord were different. Although the height-to-width ratios of the vertebral canal and spinal cord can provide an "approximate cord or canal area,"[16] results of the present study and another investigation[13] suggest that the actual measurement of the area should be used instead because that provides a more precise indication of spinal cord compression and deformation. Some measurements obtained in our study, such as the vertebral canal height, were significantly different between the clinically normal and CSM-affected Doberman Pinschers when measured in the transverse plane, but not in the sagittal plane. These discrepancies likely occurred because transverse measurements provide a more accurate representation of anatomic structures. Landmarks are more easily identified in transverse images, and those images are less affected by positioning than images in the sagittal plane.

The shape of the spinal cord of clinically normal humans has been described as a circular ellipse in the cranial cervical area and as an anteroposteriorly flattened oval ellipse in the caudal cervical area.[16] In Doberman Pinschers of the study reported here, the pattern of spinal cord shape was opposite to that of humans, but lack of data in the veterinary literature prevents comparison with findings in other breeds of dog. At the C7-T1 disk level, the spinal cord commonly had a trapezoid shape in clinically normal and CSM-affected Doberman Pinschers. This observation is clinically relevant because it could be mistaken as a bilateral dorsolateral compression causing spinal cord deformation.

Our data have indicated that clinically normal Doberman Pinchers have a high incidence of disk degeneration and protrusion, foraminal stenosis, and nonclinical spinal cord compression. Therefore, care should be exercised when attributing clinical importance to these changes in Doberman Pinschers. The combination of a relatively stenotic vertebral canal with wide intervertebral disks appears to be a key feature in the pathogenesis of CSM in Doberman Pinschers. The disk distraction measurements revealed similar intervertebral mobility between clinically normal and CSM-affected Doberman Pinschers. On the basis of these findings, it appears that a combination of static factors prevails in the initial pathogenesis of CSM in Doberman Pinchers and that cervical vertebral instability, if present, has a secondary role in the pathogenesis of CSM.

a. Sharp NJ, Cofone M, Robertson ID, et al. Cervical spondylomyelopathy in the Doberman dog: a potential model for cervical spondylotic myelopathy in humans (abstr). *J Invest Surg* 1989;2:333.
b. Burbidge HM. *Caudal cervical malformation in the Dobermann pinscher*. PhD thesis, Massey University, Aukland, New Zealand, 1999.
c. Magnetom Vision, Siemens Canada, Mississauga, ON, Canada. Signa Infinity, GE Medical Systems-Canada, Mississauga, ON, Canada.
d. Magnevist, Berlex Canada Inc, Lachine, QC, Canada.
e. DicomWorks, Lyon, France. Available at: dicom.online.fr. Accessed Jun 18, 2004.
f. SAS statistical software, version 8.2, SAS Institute Inc, Cary, NC.

References

1. VanGundy TE. Disc-associated wobbler syndrome in the Doberman pinscher. *Vet Clin North Am Small Anim Pract* 1988;18:667–696.
2. Raffe MR, Knecht CD. Cervical vertebral malformation—a review of 36 cases. *J Am Anim Hosp Assoc* 1980;16:881–883.
3. Seim HB, Withrow SJ. Pathophysiology and diagnosis of caudal cervical spondylo-myelopathy with emphasis on the Doberman Pinscher. *J Am Anim Hosp Assoc* 1982;18:241–251.
4. Read RA, Robins GM, Carlisle CM. Caudal cervical spondylo-myelopathy (wobbler syndrome) in the dog—a review of thirty cases. *J Small Anim Pract* 1983;24:605–621.
5. Lewis DG. Cervical spondylomyelopathy ('wobbler' syndrome) in the dog: a study based on 224 cases. *J Small Anim Pract* 1989;30:657–665.
6. Burbidge HM, Pfeiffer DU, Blair HT. Canine wobbler syndrome: a study of the Dobermann pinscher in New Zealand. *N Z Vet J* 1994;42:221–228.
7. Lewis DG. Cervical spondylomyelopathy ("Wobbler") syndrome in dogs. *In Pract* 1992;125–130.
8. Parker AJ, Park RD, Cusick PK, et al. Cervical vertebral instability in the dog. *J Am Vet Med Assoc* 1973;163:71–74.
9. Trotter EJ, de Lahunta A, Geary JC, et al. Caudal cervical vertebral malformation-malarticulation in Great Danes and Doberman Pinschers. *J Am Vet Med Assoc* 1976;168:917–930.
10. Jeffery ND, McKee WM. Surgery for disk-associated wobbler syndrome in the dog—an examination of the controversy. *J Small Anim Pract* 2001;42:574–581.
11. Olsson SE, Stavenborn M, Hoppe F. Dynamic compression of the cervical spinal cord. *Acta Vet Scand* 1982;23:65–78.
12. Burbidge HM, Pfeiffer DU, Guilford WG. Presence of cervical vertebral malformation in Dobermann puppies and the effects of diet and growth rate. *Aust Vet J* 1999;77:814–818.
13. Fujiwara K, Yonenobu K, Hiroshima K, et al. Morphometry of the cervical spinal cord and its relation to pathology in cases with compression myelopathy. *Spine* 1988;13:1212–1216.
14. Kameyama T, Hashizume Y, Ando T, et al. Morphometry of the normal cadaveric cervical spinal cord. *Spine* 1994;19:2077–2081.
15. Okada Y, Ikata T, Katoh S, et al. Morphologic analysis of the cervical spinal cord, dural tube, and spinal canal by magnetic resonance imaging in normal adults and patients with cervical spondylotic myelopathy. *Spine* 1994;19:2331–2335.
16. Sherman JL, Nassaux PY, Citrin CM. Measurements of the normal cervical spinal cord on MR imaging. *AJNR Am J Neuroradiol* 1990;11:369–372.
17. Tierney RT, Maldjian C, Mattacola CG, et al. Cervical spine stenosis measures in normal subjects. *J Athl Train* 2002;37:190–193.
18. Breit S, Kunzel W. Osteological features in pure-bred dogs predisposing to cervical spinal cord compression. *J Anat* 2001;199:527–537.
19. Breit S, Kunzel W. Shape and orientation of articular facets of cervical vertebrae (C3-C7) in dogs denoting axial rotational ability: an osteological study. *Eur J Morphol* 2002;40:43–51.
20. Breit S, Kunzel W. A morphometric investigation on breed-specific features affecting sagittal rotational and lateral bending mobility in the canine cervical spine (c3-c7). *Anat Histol Embryol* 2004;33:244–250.
21. Drost WT, Lehenbauer TW, Reeves J. Mensuration of cervical vertebral ratios in Doberman pinschers and Great Danes. *Vet Radiol Ultrasound* 2002;43:124–131.
22. Fourie SL, Kirberger RM. Relationship of cervical spinal cord diameter to vertebral dimensions: a radiographic study of normal dogs. *Vet Radiol Ultrasound* 1999;40:137–143.
23. Jones JC, Wright JC, Bartels JE. Computed tomographic morphometry of the lumbosacral spine of dogs. *Am J Vet Res* 1995;56:1125–1132.
24. Feeney DA, Evers P, Fletcher TF, et al. Computed tomogra-

phy of the normal canine lumbosacral spine—a morphologic perspective. *Vet Radiol Ultrasound* 1996;37:399–411.

25. Dabanoglu I, Kara ME, Turan E, et al. Morphometry of the thoracic spine in German shepherd dog: a computed tomographic study. *Anat Histol Embryol* 2004;33:53–58.

26. Hitselberger WE, Witten RM. Abnormal myelograms in asymptomatic patients. *J Neurosurg* 1968;28:204–206.

27. Teresi LM, Lufkin RB, Reicher MA, et al. Asymptomatic degenerative disk disease and spondylosis of the cervical spine: MR imaging. *Radiology* 1987;164:83–88.

28. Boden SD, McCowin PR, Davis DO, et al. Abnormal magnetic-resonance scans of the cervical spine in asymptomatic subjects. A prospective investigation. *J Bone Joint Surg Am* 1990;72:1178–1184.

29. Matsumoto M, Fujimura Y, Suzuki N, et al. MRI of cervical intervertebral discs in asymptomatic subjects. *J Bone Joint Surg Br* 1998;80:19–24.

30. da Costa RC, Poma R, Parent JM, et al. Correlation of motor evoked potentials with magnetic resonance imaging and neurologic findings in Doberman Pinschers with and without signs of cervical spondylomyelopathy. *Am J Vet Res* 2006;671613–1620.

31. McKee WM, Butterworth SJ, Scott HW. Management of cervical spondylopathy-associated intervertebral, disc protrusions using metal washers in 78 dogs. *J Small Anim Pract* 1999;40:465–472.

32. Kasai Y, Uchida A. New evaluation method using preoperative magnetic resonance imaging for cervical spondylotic myelopathy. *Arch Orthop Trauma Surg* 2001;121:508–510.

33. Lewis DG. Radiological assessment of the cervical spine of the Dobermann with reference to cervical spondylomyelopathy. *J Small Anim Pract* 1991;32:75–82.

34. Jones JC, Inzana KD. Subclinical CT abnormalities in the lumbosacral spine of older large-breed dogs. *Vet Radiol Ultrasound* 2000;41:19–26.

35. Houser OW, Onofrio BM, Miller GM, et al. Cervical spondylotic stenosis and myelopathy: evaluation with computed tomographic myelography. *Mayo Clin Proc* 1994;69:557–563.

36. Shores A. Canine vertebral malformation/malarticulation syndrome. *Compend Contin Educ Pract Vet* 1984;6:326–334.

37. Yu YL, du Boulay GH, Stevens JM, et al. Computer-assisted myelography in cervical spondylotic myelopathy and radiculopathy. Clinical correlations and pathogenetic mechanisms. *Brain* 1986;109:259–278.

38. White AA III, Panjabi MM. Biomechanical considerations in the surgical management of cervical spondylotic myelopathy. *Spine* 1988;13:856–860.

39. Bernhardt M, Hynes RA, Blume HW, et al. Cervical spondylotic myelopathy. *J Bone Joint Surg Am* 1993;75:119–128.

40. Watkins RG, Williams L, Watkins RG. Cervical spine injuries in athletes. In: Clark CR, ed. *The cervical spine*. 4th ed. Philadelphia: Lippincott Williams & Wilkins, 2005;567–586.

41. Summers BA, Cummings JF, de Lahunta A. Injuries to the central nervous system. In: Summers BA, Cummings JF, de Lahunta A, eds. *Veterinary neuropathology*. St Louis: Mosby, 1995;193–200.

42. Sharp NJH, Cofone M, Robertson ID, et al. Computed tomography in the evaluation of caudal cervical spondylomyelopathy of the Doberman Pinscher. *Vet Radiol Ultrasound* 1995;36:100–108.

43. Parke WW. Correlative anatomy of cervical spondylotic myelopathy. *Spine* 1988;13:831–837.

44. de Lahunta A. Cervical spinal cord contusion from spondylolisthesis (a wobbler syndrome in dogs). In: Kirk RW, ed. *Current veterinary therapy IV—small animal practice*. 4th ed. Philadelphia: WB Saunders Co, 1971;503–504.

45. Wright JA. A study of the radiographic anatomy of the cervical spine in the dog. *J Small Anim Pract* 1977;18:341–357.

46. Morgan JP, Miyabayashi T, Choy S. Cervical spine motion: radiographic study. *Am J Vet Res* 1986;47:2165–2169.

47. Penning L, Badoux DM. Radiological study of the movements of the cervical spine in the dog compared with those in man. *Anat Histol Embryol* 1987;16:1–20.

48. Dai L. Disc degeneration and cervical instability. Correlation of magnetic resonance imaging with radiography. *Spine* 1998;23:1734–1738.

49. Kumaresan S, Yoganandan N, Pintar FA, et al. Contribution of disc degeneration to osteophyte formation in the cervical spine: a biomechanical investigation. *J Orthop Res* 2001;19:977–984.

50. Kaigle AM, Wessberg P, Hansson TH. Muscular and kinematic behavior of the lumbar spine during flexion-extension. *J Spinal Disord* 1998;11:163–174.

51. Fehlings MG, Skaf G. A review of the pathophysiology of cervical spondylotic myelopathy with insights for potential novel mechanisms drawn from traumatic spinal cord injury. *Spine* 1998;23:2730–2737.

52. Lu J, Ebraheim NA, Huntoon M, et al. Cervical intervertebral disc space narrowing and size of intervertebral foramina. *Clin Orthop Relat Res* 2000;370;259–264.

53. Finelli DA, Hurst GC, Karaman BA, et al. Use of magnetization transfer for improved contrast on gradient-echo MR images of the cervical spine. *Radiology* 1994;193:165–171.

54. Held P, Seitz J, Frund R, et al. Comparison of two-dimensional gradient echo, turbo spin echo and two-dimensional turbo gradient spin echo sequences in MRI of the cervical spinal cord anatomy. *Eur J Radiol* 2001;38:64–71.

55. Melhem ER, Bert RJ, Faddoul SG. Cervical spondylosis: contrast-enhanced magnetization transfer prepulsed 3D turbo field echo MR imaging. *J Magn Reson Imaging* 2000;11:294–298.

56. Humphreys SC, Hodges SD, Patwardhan A, et al. The natural history of the cervical foramen in symptomatic and asymptomatic individuals aged 20-60 years as measured by magnetic resonance imaging. A descriptive approach. *Spine* 1998;23:2180–2184.

57. Ebraheim NA, An HS, Xu R, et al. The quantitative anatomy of the cervical nerve root groove and the intervertebral foramen. *Spine* 1996;21:1619–1623.

58. Sohn HM, You JW, Lee JY. The relationship between disc degeneration and morphologic changes in the intervertebral foramen of the cervical spine: a cadaveric MRI and CT study. *J Korean Med Sci* 2004;19:101–106.

59. Yoo JU, Zou D, Edwards WT, et al. Effect of cervical spine motion on the neuroforaminal dimensions of human cervical spine. *Spine* 1992;17:1131–1136.

60. Kitagawa T, Fujiwara A, Kobayashi N, et al. Morphologic changes in the cervical neural foramen due to flexion and extension: in vivo imaging study. *Spine* 2004;29:2821–2825.

61. Lipsitz D, Levitski RE, Chauvet AE, et al. Magnetic resonance imaging features of cervical stenotic myelopathy in 21 dogs. *Vet Radiol Ultrasound* 2001;42:20–27.

62. Bucciero A, Vizioli L, Tedeschi G. Cord diameters and their significance in prognostication and decisions about management of cervical spondylotic myelopathy. *J Neurosurg Sci* 1993;37:223–228.

63. da Costa RC, Pippi NL, Graça DL, et al. The effects of free fat graft or cellulose membrane implants on laminectomy membrane formation in dogs. *Vet J* 2006;171:491–499.